Deep-Sea Research II 53 (2006) 1241–1260

DEEP-SEA RESEARCH
PART II

www.elsevier.com/locate/dsr2

Spatial and temporal variability of phytoplankton in the Gulf of Cádiz through remote sensing images

Gabriel Navarro[a,b,*], Javier Ruiz[a]

[a]Departamento de Oceanografía, Instituto de Ciencias Marinas de Andalucía, Consejo Superior de Investigaciones Científicas, 11510 Puerto Real, Cádiz, Spain

[b]Departamento de Biología, Facultad de Ciencias del Mar y Ambientales, Universidad de Cádiz, 11510 Puerto Real, Cádiz, Spain

Received 1 February 2005; accepted 10 April 2006

Abstract

The temporal and spatial distribution of chlorophyll concentration in the Gulf of Cádiz (SW Spain) was analysed between 1998 and 2002 by remote sensing data from the Sea-viewing Wide Field-of-view Sensor (SeaWiFS). Climatological and monthly averages showed the presence of more productive waters in the inner shelf of the basin, especially during spring and fall, according to the phytoplankton blooms observed. This pattern was further confirmed by the modes obtained with an Empirical Orthogonal Function (EOF) decomposition of weekly chlorophyll composite images performed for the whole period. The first EOF mode explained 20% of the variability and corresponded to the chlorophyll seasonality in the basin. The second EOF mode accounted for 10% of the variability and distinguished several regions with different oceanographic features in the area. Five zones could be identified among which, a coastal zone between Huelva and Cádiz, was found to show the highest chlorophyll concentration values. Local zonal winds, categorized as westerlies and easterlies, were coupled with differences in biological production. The former induced an increase in chlorophyll concentration whereas the latter caused a decrease in phytoplankton biomass. Rainfall and river discharge also affected markedly the chlorophyll concentration.

Keywords: Gulf of Cádiz; SW Spain; SeaWiFS; Chlorophyll patterns; AVHRR; EOF

1. Introduction

The Gulf of Cádiz (Fig. 1) is a wide basin located west of the Strait of Gibraltar between the Iberian Peninsula and the African continent. Surface waters from the North Atlantic feed the Mediterranean through the Strait after crossing this basin. The flux of Atlantic waters affects the oceanographic characteristics of surface waters in the Gulf and plays an important role in the regulation of circulation in the Mediterranean basin. However, little is known of surface dynamics in the Gulf since most of oceanographic research carried out in the basin has been focused on the study of the deep Mediterranean outflow (Baringer and Price, 1999) whose impact on upper waters is limited since it occurs at several hundreds meters depth.

Nevertheless, surface dynamics in the basin are diverse as evidenced from a few studies performed

*Corresponding author. Tel.: +34 956 832612; fax: +34 956 834701.
E-mail address: gabriel.navarro@icman.csic.es (G. Navarro).

0967-0645/$ - see front matter © 2006 Elsevier Ltd. All rights reserved.
doi:10.1016/j.dsr2.2006.04.014

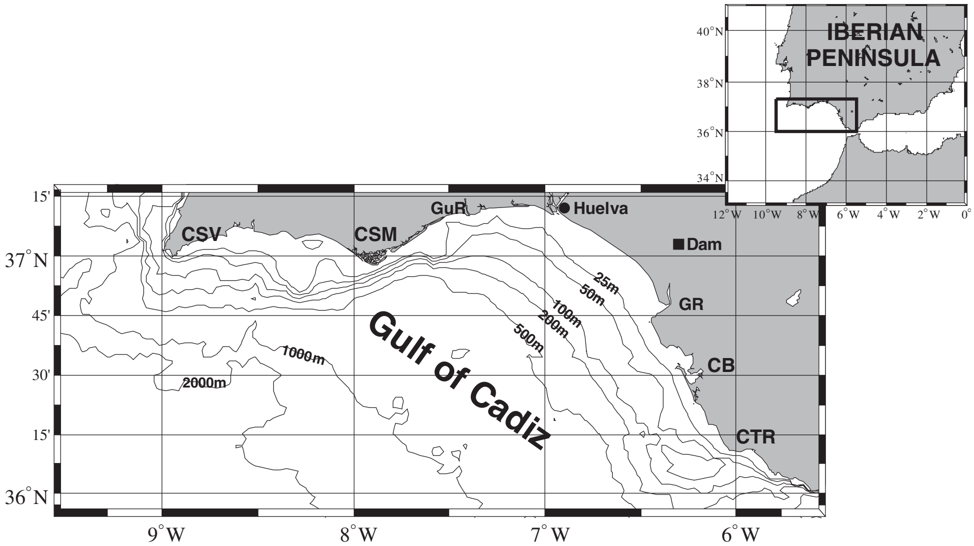

Fig. 1. Bathymetry and location map of the Gulf of Cádiz (square indicates the study area) sited in SW Spain. Letters indicate locations and geographic regions referred in the text: CSV-Cape San Vicente; CSM-Cape Santa María; GuR-Guadiana River; GR-Guadalquivir River; CB-Cádiz Bay; CTR-Cape Trafalgar, Huelva meteorological station (circle symbol) and Alcalá del Río dam. The black lines represent the bathymetry (25, 50, 100, 200, 500, 1000 and 2000 m).

aimed at identifying patterns from thermal images in conjunction with in situ measurements (Stevenson, 1977; Fiúza et al., 1982; Fiúza, 1983; Folkard et al., 1997; Vargas et al., 2003; Relvas and Barton, 2002; García-Lafuente et al., 2006; Criado-Aldeanueva et al., 2006). These studies have evidenced the existence of different structures in the Gulf: (i) a warm–cold–warm structure heading southeastward of Cape Santa María, namely the Huelva Front (Stevenson, 1977); (ii) areas of intense upwelling in the proximities of Cape San Vicente; and (iii) mixing zones at Cape Trafalgar (Fiúza et al., 1982; Fiúza, 1983; Folkard et al., 1997). These descriptive studies have been examined statistically through an Empirical Orthogonal Function analysis (EOF) of a long historical set of thermal images (Vargas et al., 2003). The analysis allowed the identification of a very stable, warm, anti-cyclonic circulation feature in the central part of the basin and another feature at the Iberian shelf, the presence of a fringe of coastal waters located between the Guadalquivir and Guadiana rivers. This fringe has a thermal characteristic, since Sea Surface Temperature (SST) is observed to be warmer with respect to rest of the basin in summer and colder in winter. Recent studies (García-Lafuente et al., 2006) have shown that the heating of waters near the Guadalquivir River mouth may cause the generation of a counter current detected in this area in the summer season.

Although all these oceanographic structures have been described in the basin, the majority of studies have been exclusively based on the analysis of thermal images of the Advanced Very High Resolution Radiometer (AVHRR) sensor but the influence of these structures on the spatial–temporal distributions of chlorophyll in the Gulf has not been examined. Only a few studies that use ocean colour images have been reported. Through daily images of Coastal Zone Colour Scanner (CZCS) sensor, Sousa and Bricaud (1992) precisely illustrated some pigment patterns in the Gulf of Cádiz, for example filaments in the vicinity of Cape San Vicente. In addition, Peliz and Fiúza (1999) presented a complete study on the spatial-temporal variability of surface pigments derived from CZCS around the entire Portuguese coast, which briefly included the Gulf of Cádiz.

The aim of this work was to perform the first combined analysis of both SST and surface chlorophyll concentration estimated from remote sensors between 1998 and 2002 in order to examine the physical and biological coupling in the Gulf of Cádiz. Based on the correlation found between the different patterns of variability and the oceanographic features, several zones are identified and described in the basin.

2. Methods

2.1. Remote sensing images

The analysis was carried out using AVHRR and Sea-viewing Wide Field of view Sensor (SeaWiFS) images. Thermal images were accessible via ISIS and EOWEB on the German Remote Sensing Data Center website (DLR, Deutsches Zentrum für Luft- und Raumfahrt). Daily maps of SST were composed using up to five different NOAA (National Oceanic and Atmospheric Administration) acquisitions. Weekly and monthly composite images were produced by averaging the temperature of the corresponding daily composites at each pixel. The spatial resolution was set as 1.1 km at the nadir. The details of navigation, calibration, cloud screening and algorithms can be seen at www.isis.dlr.de. The method used to calculate the temperature is based on the "Split Window Technique" algorithm, proposed by McClain et al. (1985). The radiometric resolution of the SST images was 8 bits. Value 0 refers to "earth", and the 255 values correspond to "clouds". Temperature ranged from 0.125 to 31.75 °C, divided in 254 intervals. The digital number was multiplied by 0.125 to obtain the temperature value in degree Celsius. The images were projected in Mercator projection using M_Map v1.3 toolbox for Matlab written by Rich Pawlowicz (www.eos.ubc.ca/~rich/map.html).

SeaWiFS instrument was launched on 1 August 1997, and the first data were collected on September 4th. We used daily SeaWiFS local area coverage (LAC) data received by the satellite ground receiving station at the University of Las Palmas de Gran Canaria (HCAN) at 1.1 km spatial resolution. These images, high-resolution level 1 SeaWiFS ocean colour radiances, were atmospherically corrected and processed to level 2 using SeaDAS version 4 (www.seadas.gsfc.nasa.gov). SeaDAS also was used to remap (Mercator projection) level-2 chlorophyll concentration and PAR (Photosynthetic Available Radiation) estimation. Each image was navigated, if necessary, by co-registering the image with the outline of the coast. In SeaDAS, chlorophyll concentration is derived from the OC4 ocean colour algorithm (O'Reilly et al., 1998, 2000). The accuracy of water-leaving radiances measured by SeaWiFS is within 5%, and chlorophyll-*a* derived from the data is within 35% for case-I waters (McClain et al., 1995).

Weekly and monthly chlorophyll and PAR composites were formed by arithmetically averaging all daily available scenes each week and month respectively, on a pixel-by-pixel basis. Valid pixels were those whose chlorophyll concentrations varied from 0.01 to 10 mg Chl m^{-3}; e.g., excluding missing data, clouds, and extremely high chlorophyll values (which are not usually observed in the area; Navarro et al., 2006; Sánchez-Lamadrid et al., 2003). The spatial resolution on the input images (1.1 km) was retained in the resulting weekly and monthly means of SeaWiFS images. A total of 1216 daily SeaWiFS images were available from January 1998 through December 2002.

To investigate the quality of the SeaWiFS chlorophyll data in the study area and considering that OC4 algorithm could overestimate high chlorophyll concentration in areas located very close to the coast (Lavender et al., 2004), chlorophyll concentration at 10 m water depth was measured during GOLFO 2001 cruise (Navarro et al., 2006) or obtained from available data of several oceanographic cruises (TOFIÑO and RESERVA, Navarro, 2004) and subsequently compared with the remote sensing results. The correlation found between both procedures was statistically significant ($r = 0.85$, $p < 0.001$ and $n = 304$, Fig. 2). Chlorophyll was measured

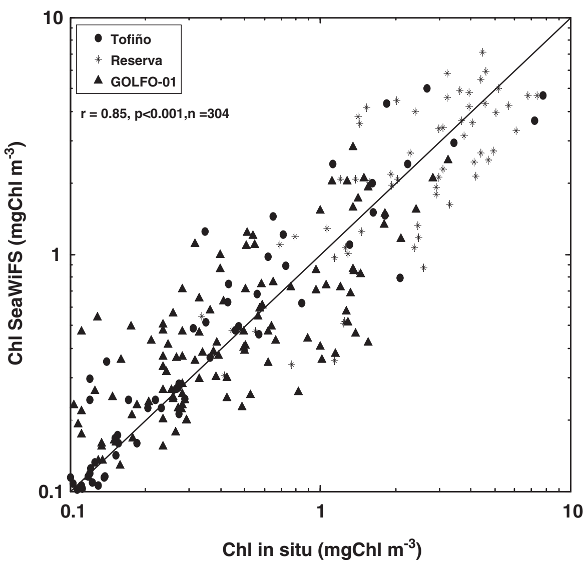

Fig. 2. Comparison between the chlorophyll concentrations (mg Chl m^{-3}) provided by SeaWiFS and in situ measurements at 10 m obtained during several cruises: Tofiño (September and October 2000), GOLFO-01 (May–June 2001) and RESERVA (several cruises in November 2001, December 2001, January 2002 and April 2002).

fluorometrically with a Turner Designs fluorometer according to UNESCO (1994) in samples taken the same day of the data sensor acquisition, although the difference between the collection and data acquisition by the sensor could differ, which could introduce some noise in the correlation.

2.2. Wind and rain data

Wind and rain data were obtained from a nearby meteorological station located at Huelva (Fig. 1) of the Instituto Nacional de Meteorología. The sampling interval was 1 h for wind data and 1 day for rain data. The data were filtered with a low-pass filter with cut-off at a period of 3 days, in order to have similar smoothness for the wind series as for the weekly time series that are described below.

2.3. EOF analysis

EOF analysis is a statistical method that compresses the variability in a time-series data with the aim at providing a compact description of their spatial–temporal variability in terms of orthogonal functions. This method of data reduction was first applied by Lorenz (1956) to geophysical records for the purpose of statistical weather prediction. Related to ocean-colour data, there are many examples in the literature concerning EOF analysis of chlorophyll images (e.g., Baldacci et al., 2001; Yoder et al., 2001; Palacios, 2004; Ho et al., 2004; Brickley and Thomas, 2004).

In this work, singular value decomposition (SVD) was used to carry out the EOF analysis. The method allows obtaining the orthogonal functions as well as the eigenvalues and the amplitudes (Kelly, 1988). The data matrix $D_{(x,t)}$, is composed by m rows (number of pixels in each image) and n columns (number of images in time), and can be written as the product of three matrices:

$$D = USV^{\mathrm{T}}. \quad (1)$$

The SVD of a matrix D decomposes the matrix into two orthogonal matrices U and V whose columns consist of the left and right singular vectors. The eigenvalues are also present in the decomposition as elements of a diagonal matrix (S), and determine the percentage of the variance that explains each mode. We can calculate the effect of a given EOF mode on the data for a certain time by multiplying the spatial EOF patterns by the amplitude in the temporal mode for the time of interest.

The SVD method requires a data set without gaps. Therefore, those images with more than 10% of cloud pixels were rejected. Due to this correction, the original number of weekly composites, 260 (5 years) resulted finally in a reduction to 196 weekly composites (Fig. 3). For valid images, pixels covered by clouds were replaced by the average of the surrounding pixels (3×3 box). Data were normalized dividing each pixel by the standard deviation of

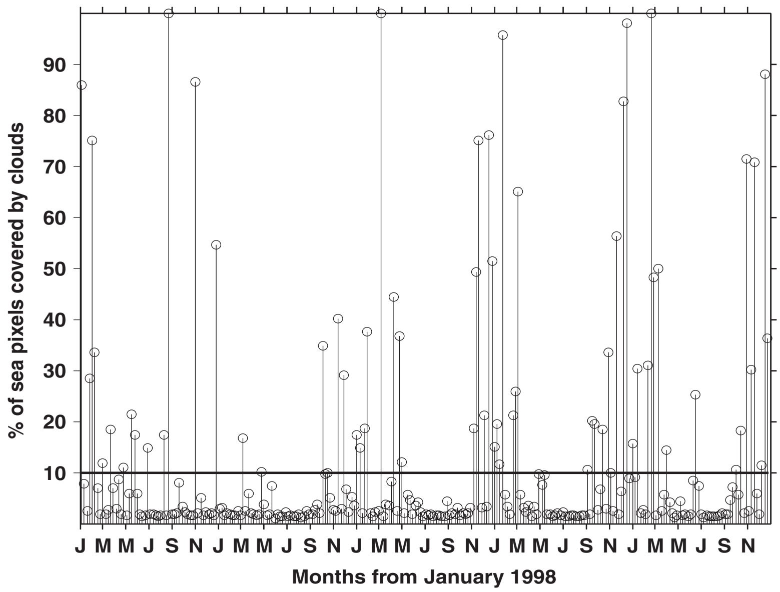

Fig. 3. Percentage of cloudy "sea" pixels versus chlorophyll weekly composite. The horizontal solid line indicates 10% of cloud coverage.

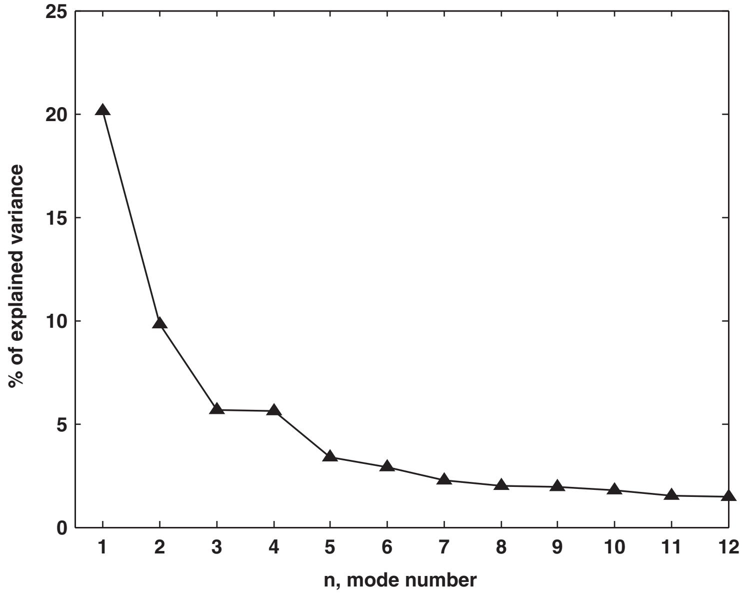

Fig. 4. Percentage of variance explained by the EOF modes 1–3, explaining 20%, 9.8% and 5.6% of the variance, respectively.

the time series (Davis, 1973). EOF analysis was performed after subtracting the temporal mean of each pixel. This particular EOF is called ‘‘temporal EOF’’ (Lagerloef and Bernstein, 1988), and some authors suggest that this method is more appropriate when analysing structures associated with the seasonal variability in the area (Parada and Canton, 1998; Baldacci et al., 2001).

The errors produced in the account of the EOF due to the finite number of images used in the method can be estimated. Following North et al. (1982), the ‘‘error distance’’ $\delta\lambda$ is given by

$$\delta\lambda \approx \lambda\left(\frac{2}{n}\right)^{1/2}, \quad (2)$$

where λ is the eigenvalues and n is the number of images used in the EOF analysis. In our study, n was 196 images, so $\delta\lambda \approx 0.1010$. A mode is considered significant only if the distance between λ and its nearest eigenvalues is bigger than the error associated with its eigenvalues $\delta\lambda$. In our study, only the first two modes were found significant.

3. Results

The results of the EOF analysis performed on the weekly chlorophyll images are shown in Figs. 4–6. The percentage distribution of the normalized variance explained by the higher modes is shown in Fig. 4. The first two modes explained 20% and

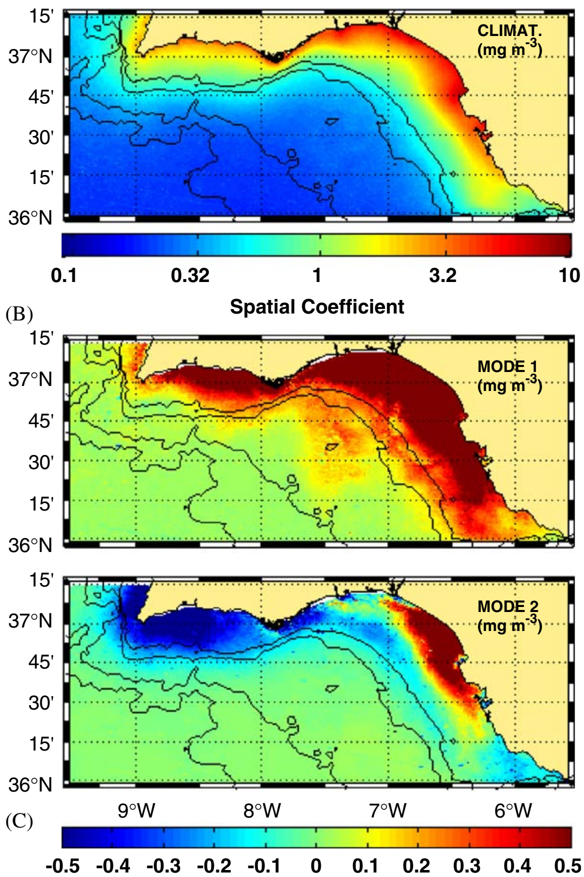

Fig. 5. (A) Monthly climatology of SeaWiFS chlorophyll ($mg\,Chl\,m^{-3}$). Spatial coefficients maps correspond to the first (B) and second (C) mode.

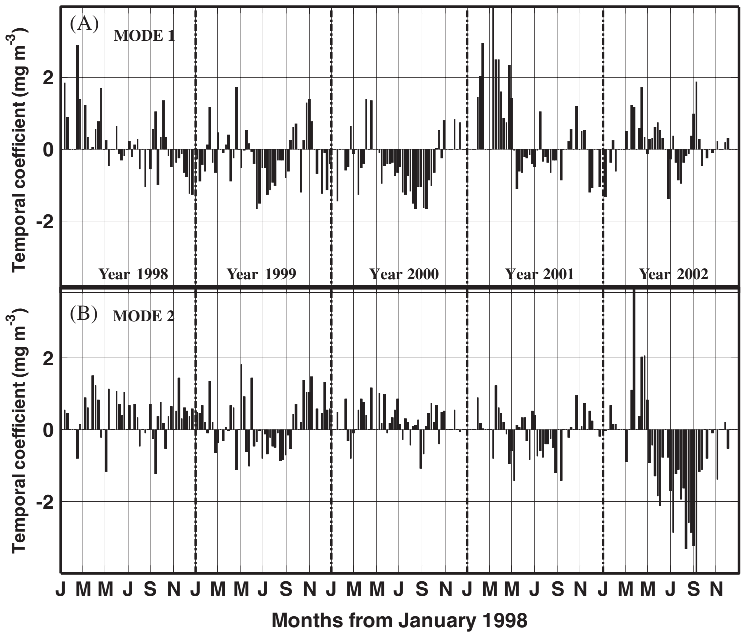

Fig. 6. Time series of the amplitude of the first two EOF modes.

10% of the normalized variance, respectively. Spatial coefficients of the two first modes represent the spatial extension and the dynamic importance of the processes in the study area (Fig. 5(B)–(C)). The intensity of the phenomenon is directly related to the amplitude of the spatial coefficient. With respect to the temporal amplitude, the temporal EOF mode indicates the importance of the phenomenon (Fig. 6). Therefore, the combination of the spatial and temporal variability can be obtained multiplying the spatial coefficient by the temporal amplitude. For our results, only the first two modes were found to be statistically significant and further considered to explain the chlorophyll variability. Almost 30% of such variability could be explained by these two modes (Fig. 4). The first mode was responsible for 20% of the normalized variance and seems to be related to the seasonality of phytoplankton blooms. Most of the spatial coefficients were positive (Fig. 5(B)), being maxima in a coastal fringe coinciding spatially with the maxima values of chlorophyll concentration presented in the area (Fig. 5(A)). Consequently, when they were multiplied by positive temporal amplitudes the whole field increased with respect to the chlorophyll climatology and viceversa-negative amplitudes resulted in a decrease of the field. The temporal amplitude had positive values in spring and fall, whereas negative values were obtained in summer and winter. Monthly time series of chlorophyll concentration for the whole area also exhibits these patterns (Navarro, 2004). According to the monthly climatology, the maximum value of the temporal amplitude was reached in spring 2001 (4 March 2001).

The second mode explained 9.8% of the normalized variance (Fig. 4). Spatial distribution of this mode and the previous knowledge of the area (Stevenson, 1977; Fiúza et al., 1982; Fiúza, 1983; Folkard et al., 1997; Vargas et al., 2003; Relvas and Barton, 2002) allow us to distinguish different zones throughout the basin (Fig. 7). The first zone (Zone 1; Fig. 7) was located in the open ocean, being characterized by values of the spatial coefficient near 0, which indicates a high stability of the surface chlorophyll with respect to the rest of the Gulf. The second area (Zone 2; Fig. 7) corresponded with the region influenced by the hydrodynamics of Cape San Vicente. The spatial coefficients were negative (around −0.5), suggesting the existence of a phytoplankton bloom when the temporal amplitude was also negative. The third zone identified (Zone 3; Fig. 7) situated east of Cape Santa María, also displayed negatives spatial coefficients. This area could be associated with the system formed by waters at the so-called ‘‘Huelva Front’’ (Stevenson, 1977). Negative values were also found close to Cape Trafalgar (Zone 5; Fig. 7), where the presence

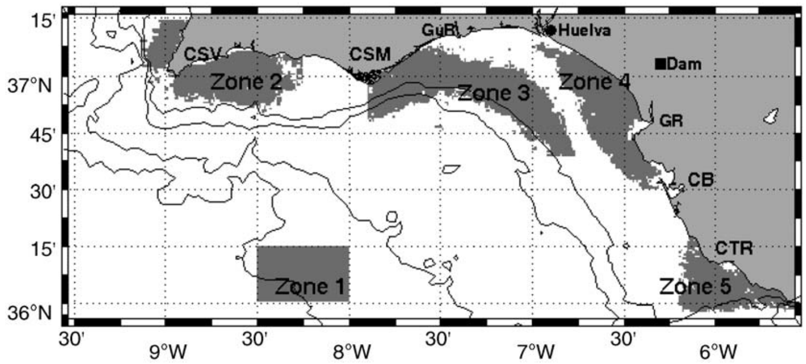

Fig. 7. Study areas distinguished by the second EOF mode: Zone 1 (open ocean), Zone 2 (Cape San Vicente), Zone 3 (Cape Santa María), Zone 4 (coastal zone between Guadiana and Guadalquivir river mouths), and Zone 5 (Cape Trafalgar). Further details are given in the text.

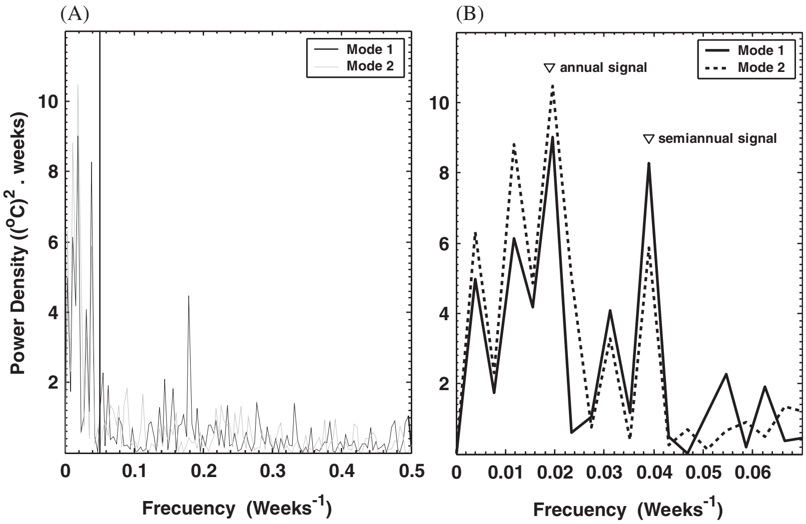

Fig. 8. The power spectrum ((mg Chl m^{-3})^2 weeks) of the temporal coefficients of the first two EOF modes. Frequency axis (in weeks^{-1}) varies between 0 and 0.5 wk^{-1} (A) and 0 and 0.06 wk^{-1} (B).

of chlorophyll-rich and cold waters has been previously reported (Prieto et al., 1999; Vargas-Yáñez et al., 2002; García et al., 2002). In contrast, the Zone 4 (Fig. 7), which occupies a coastal area located between Huelva and Cádiz, was characterized by positive spatial modes, which indicates a dynamical response of different phase compared to the remaining zones.

A spectral analysis carried out on the temporal amplitudes of the two first modes (Fig. 8) showed the dominance of the annual signal (0.02 wk^{-1}), while the semiannual signal (0.04 wk^{-1}) seemed to constitute the greater signal in intrannuals variations. In a study using CZCS images, Peliz and Fiúza (1999) also found that the annual signal dominated over the rest of signals, with the semiannual dominating in the intrannual period.

3.1. Study of the different zones delimited by the EOFs

As indicated in the previous section, several zones displaying distinct surface chlorophyll patterns could be identified by the second spatial mode. In order to study in details the temporal variability of these patterns in all zones, different remote sensing variables found in each zone were selected and analysed, including meteorological forcing factors obtained from the Huelva meteorological station.

3.1.1. Zone 1 or oceanic zone

The open-ocean zone (Zone 1; Fig. 7) occupies an area of a bathymetry deeper than 1000 m, thereby the topography factor is not expected to greatly influence the physical and biological features. Fig. 9 shows the monthly climatology and the anomalies at different years for the SST, PAR and chlorophyll concentration. The temporal series of PAR and SST have a clear seasonality, with a 3-months phase lag between them. The maxima of PAR and SST occurred in June (60 mol quanta $m^{-2} d^{-1}$) and September ($\approx$22.5 °C), respectively, whereas the minima were reached in December ($\approx$19 mol quanta $m^{-2} d^{-1}$) and February ($\approx$16.5 °C), respectively. The interannual variabilites for PAR and SST were very low, since the anomalies did not differ more than 5% and 10% with respect to the mean values, respectively.

The temporal monthly chlorophyll series exhibited a maximum in winter (February–March) and a minimum in summer (August–September). Chlorophyll concentration fluctuated between 0.1 and 0.5 mg Chl m^{-3} over the year, with an average concentration of 0.2 mg Chl m^{-3}, typical for oligotrophic waters. Highest anomalies were observed during the winter months, between January and March, decreasing in summer. Maximum values of chlorophyll concentration were reached in February 2000, coinciding with the SST minima. During April 2002, SST diminished compared to that detected the same month of the rest of years, in correspondence with high chlorophyll concentration values.

3.1.2. Zone 2 or zone near Cape San Vicente

SST and chlorophyll climatologies (Fig. 10) displayed remarkable differences with respect to the oceanic zone. Monthly SST variations are not as smooth as in the previous zone, unlike the PAR radiation (data not shown), suggesting that changes in temperature also were influenced by other dynamical factors. Minimum and maximum values were reached during the same months as in the previous zone, although the magnitude of SST was smaller. SST anomalies were greater in this zone, especially in summer months, when the presence of an upwelling in Cape San Vicente has been described (Fiúza, 1983).

Chlorophyll climatology presented two maxima throughout the year. The first one took place in spring and can be related to the development of spring blooms in these latitudes (Longhurst, 1995,

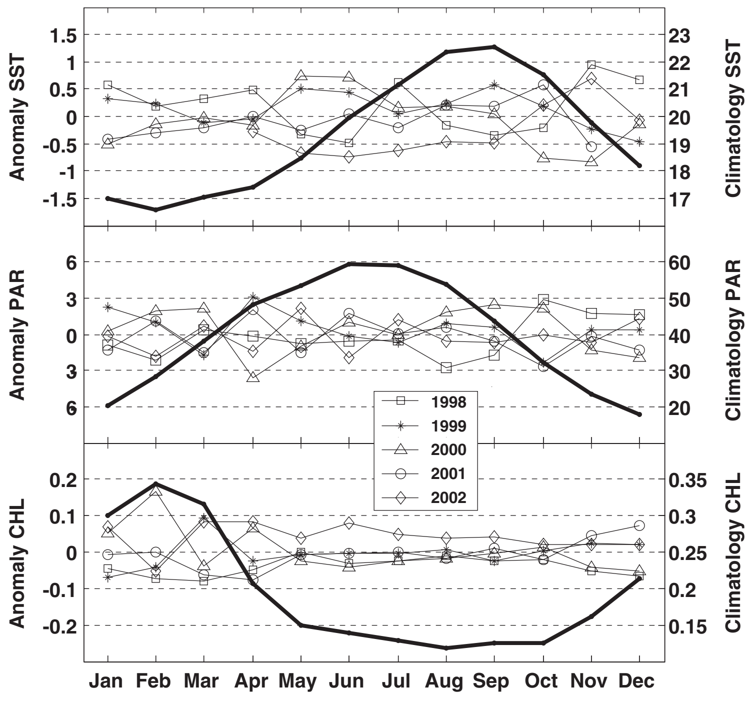

Fig. 9. Anomalies and climatology of SST (°C, top panel), PAR (mol quanta $m^{-2} d^{-1}$, central panel) and chlorophyll (mg Chl m^{-3}, bottom panel) of monthly composites between January 1998 and December 2002 for Zone 1. Climatology has been emphasized by the thick solid line.

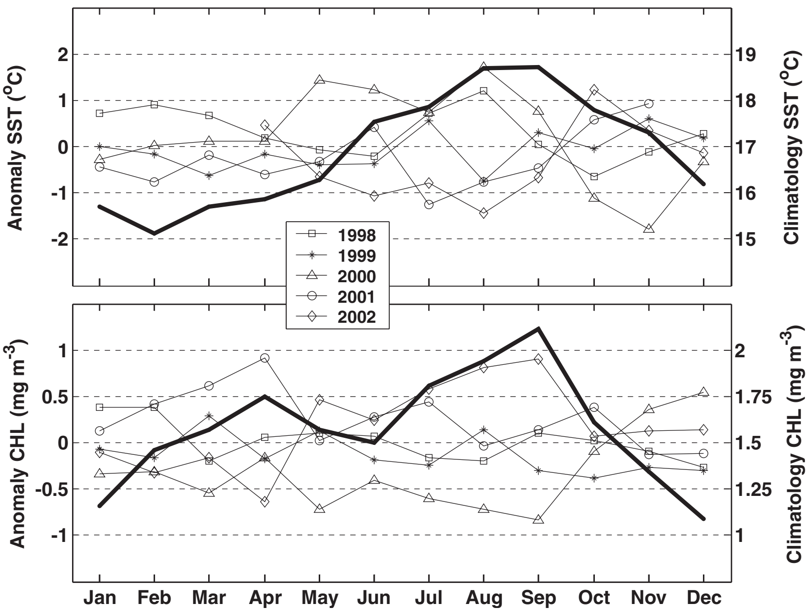

Fig. 10. Anomalies and climatology of SST (°C, top) and chlorophyll (mg Chl m^{-3}, bottom) of monthly composites between January 1998 and December 2002 for Zone 2. Climatology has been emphasized by the thick solid line.

1998). However, a second maximum of a greater intensity appeared in summer (July–September), possibly due to the upwelling processes that occur in the zone during this season (Fiúza, 1983). The relation between upwelling processes (decrease of temperature) and increased chlorophyll concentration was evident during summer. The maximum chlorophyll climatology in this zone was detected in summer 2002, coinciding with the lowest temperature record for the period considered (Fig. 10).

Fig. 11 depicts the weekly mean of SST, PAR and chlorophyll concentration for Zone 2, along with the direction and intensity of the zonal wind and also the daily precipitation. For every year, some periods show a decrease in SST in parallel with a rise in chlorophyll concentration. This situation is usually associated with the occurrence of westerlies, since these winds favour the appearance of upwelling events along the southern coast of Spain. Nonetheless, north winds also exert a great influence on the generation of upwelling processes in the area (Fiúza, 1983). As an example, in April 1998 and under the predominance of westerlies a drop in SST and an augment of chlorophyll concentration occurred. Once the westerlies disappeared, easterlies blew during the beginning of May, which originated an increase in SST and a diminution in chlorophyll concentration. In June and September, under conditions of stratification of the water column, this pattern was clearly repeated. Similarly, several examples can be described in the following years.

The fact that the highest chlorophyll concentrations were measured over summer when the radiation is maximal, indicates that this zone is not strongly limited by nutrients during this period of the annual cycle. Therefore, due to the upwelling occurring in the zone, nutrients do not limit the production during the months of maximum stratification in the basin, unlike in the oceanic zone, where the minima of surface chlorophyll were reached in summer, when the stratification of the water column is maximal and the entrance of nutrients in shallow layers is restricted.

3.1.3. Zone 3 or zone near Cape Santa María

In Zone 3, monthly SST climatology (Fig. 12) displayed the same seasonality as in the previous zones, but here the SST maximum was detected in August. The value of the maximum was intermediate between those found in Zones 1 and 2.

Fig. 12 also presents monthly chlorophyll averages. The highest concentration was observed in February, and a second maximum of a smaller intensity appeared in September, although in general the interannual variability of the maximum in winter was very high. Overall, the chlorophyll

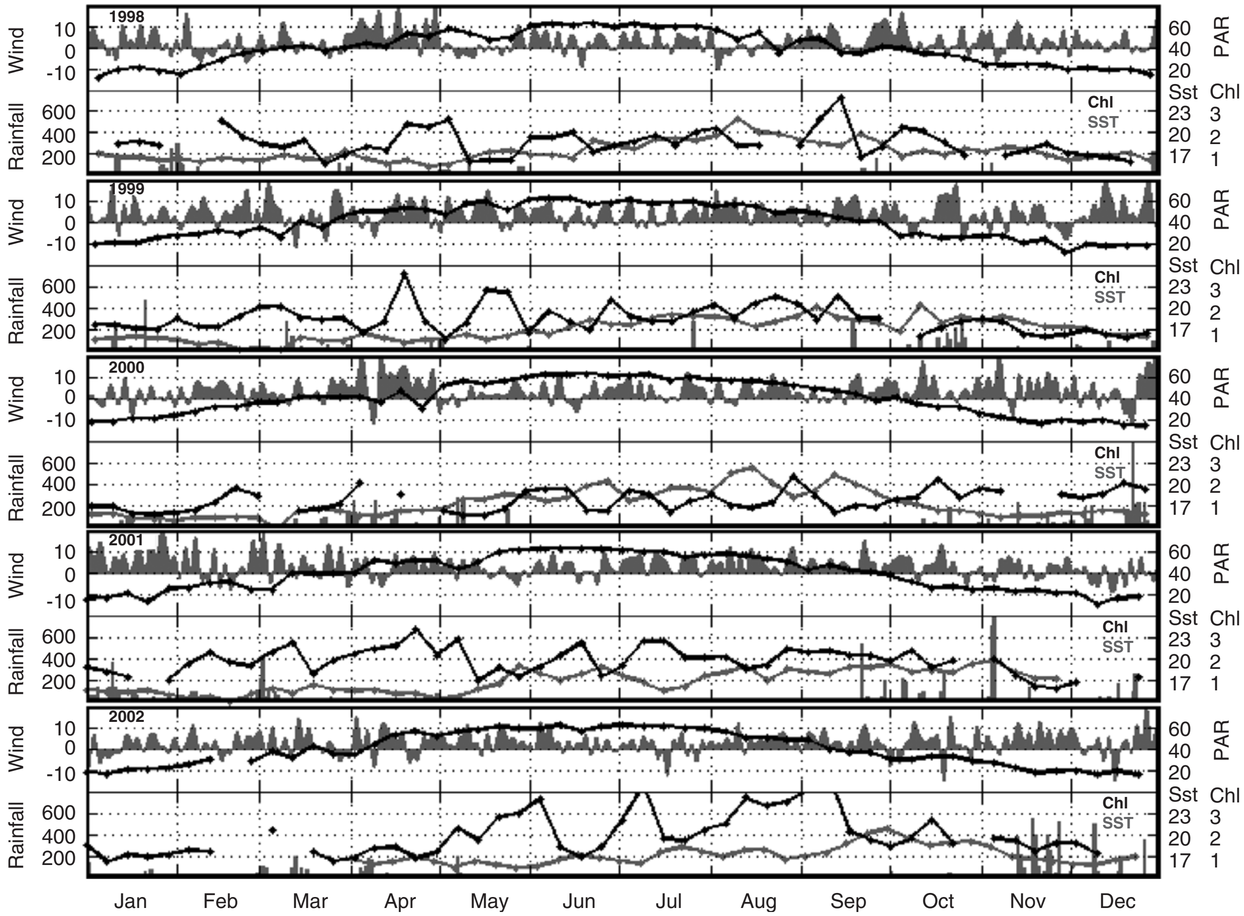

Fig. 11. Time series of local wind speed (grey bar) expressed as $km\,h^{-1}$ (positive values denotes westerlies and negative values correspond to easterlies) and PAR values (solid black line) in mol quanta $m^{-2}\,d^{-1}$ for the weekly composite in Zone 2 (top). Daily rainfall values (grey bar) in tenth $mm\,d^{-1}$ and chlorophyll concentration (black solid line) in $mg\,Chl\,m^{-3}$ and SST (grey solid line) in °C for weekly composite for Zone 2 (bottom).

concentration in this zone was smaller than in Zone 2. During April and until summer, monthly anomalies for the chlorophyll diminished and from August to September a second and high anomaly occurred. In 1998, chlorophyll maxima were achieved in February and October, whereas in 1999 they appeared in March and September. This pattern changed in 2000, with the concentration increasing from September to March 2001, when the highest maximum for the 5 years considered was obtained ($2.7\,mg\,Chl\,m^{-3}$). These results coincide with the SST minimum. In 2002, the maximum was achieved in September ($1.7\,mg\,Chl\,m^{-3}$). The chlorophyll climatology varied between 0.8 and $1.6\,mg\,Chl\,m^{-3}$, with a mean value of $1.1\,mg\,Chl\,m^{-3}$, slightly smaller that in Zone 2. Difference in the regime of zonal winds could explain this variability.

During the stratification period between April and October (Sánchez-Lamadrid et al., 2003), an increase in surface chlorophyll concentration occurred concomitantly with a decrease in SST (Fig. 13). This process took place again when westerlies blew (Fig. 13, September 1998). On the other hand, when the wind switched to easterlies, a drop in the chlorophyll concentration and an increase in surface temperature were observed (Fig. 13, April and September 1999). During August 2000, with easterlies blowing, the water warmed up due to down-welling processes and the chlorophyll decreased again. In middle August, the wind switched back to westerlies, causing a fall in temperature and a rise in chlorophyll. More examples of this situation could be observed during 2001, in particular in April, end of June and middle August as well as in 2002 at the beginning of June, middle July and beginning of September.

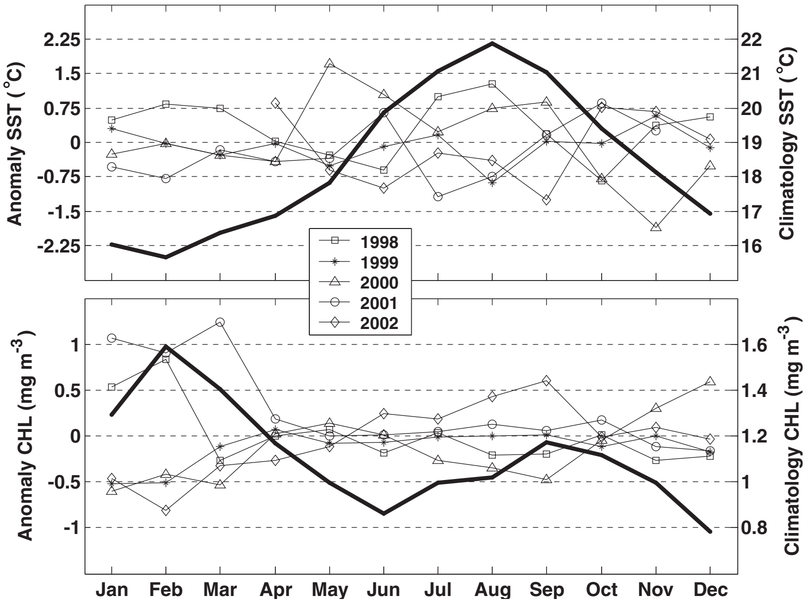

Fig. 12. Anomalies and climatology of SST (°C, top) and chlorophyll (mg Chl m^{-3}, bottom) of monthly composites between January 1998 and December 2002 for Zone 3. Climatology has been emphasized by the thick solid line.

3.1.4. Zone 4 or coastal zone between Guadiana and Guadalquivir river mouths

In this zone monthly SST climatology showed the same pattern as in the previous zones (Fig. 14), but in this case the maxima of temperature were reached in August (>23 °C) as in Zone 3, being the highest temperature climatology for all the areas. In addition, the lowest temperature value compared to the rest of areas was reached in January, indicating that in this coastal sector the range of temperature variation is the greatest for the whole Gulf. The anomalies usually fluctuated ± 1 °C, this range being smaller than in the previous zones and demonstrating a lower interannual variability.

In this coastal area the highest chlorophyll concentration was reached in April, displaying a pattern with two maxima in monthly climatology. This feature was also found in Zone 3 although the maximum chlorophyll concentration in Zone 4 was displaced 2 months with respect to the former. A second phytoplankton bloom appeared in fall, coinciding with the disappearance of the thermal stratification in October (Sánchez-Lamadrid et al., 2003).

The anomalies represented a high percentage of the average value of chlorophyll ($\approx$30%), which indicates a high interannual variability. In 1998, three chlorophyll maxima appeared; the first one was detected between January and April, the second between June and July and the last one between September and October. During 1999, chlorophyll maxima were reached in May and November, characterized by greater concentrations. This pattern changed in 2000, with maximum chlorophyll concentration in April and minimum in September, with this concentration increasing until March 2001. Moreover, another chlorophyll maximum was observed in October 2001, similar to that found in April 2002.

Fig. 15 shows weekly averages of SST, PAR and chlorophyll concentration in Zone 4. A strong visual relationship between chlorophyll increases and SST decreases was found. The fluctuations were generated when westerlies blew over the stratification period that includes the months comprised between April and October (Sánchez-Lamadrid et al., 2003). As an example, in March 1998, the predominant westerlies caused a drop in SST and a rise in chlorophyll concentration. Similarly, in the following years, several examples can be described throughout the years. In contrast, easterlies produced the opposite effect, as that registered in other zones.

Chlorophyll concentration seems to be affected by the level of precipitation in this zone. In fall, chlorophyll concentration increased in rainy years. At the end of October and beginning of November 1999, a high increase in chlorophyll concentration

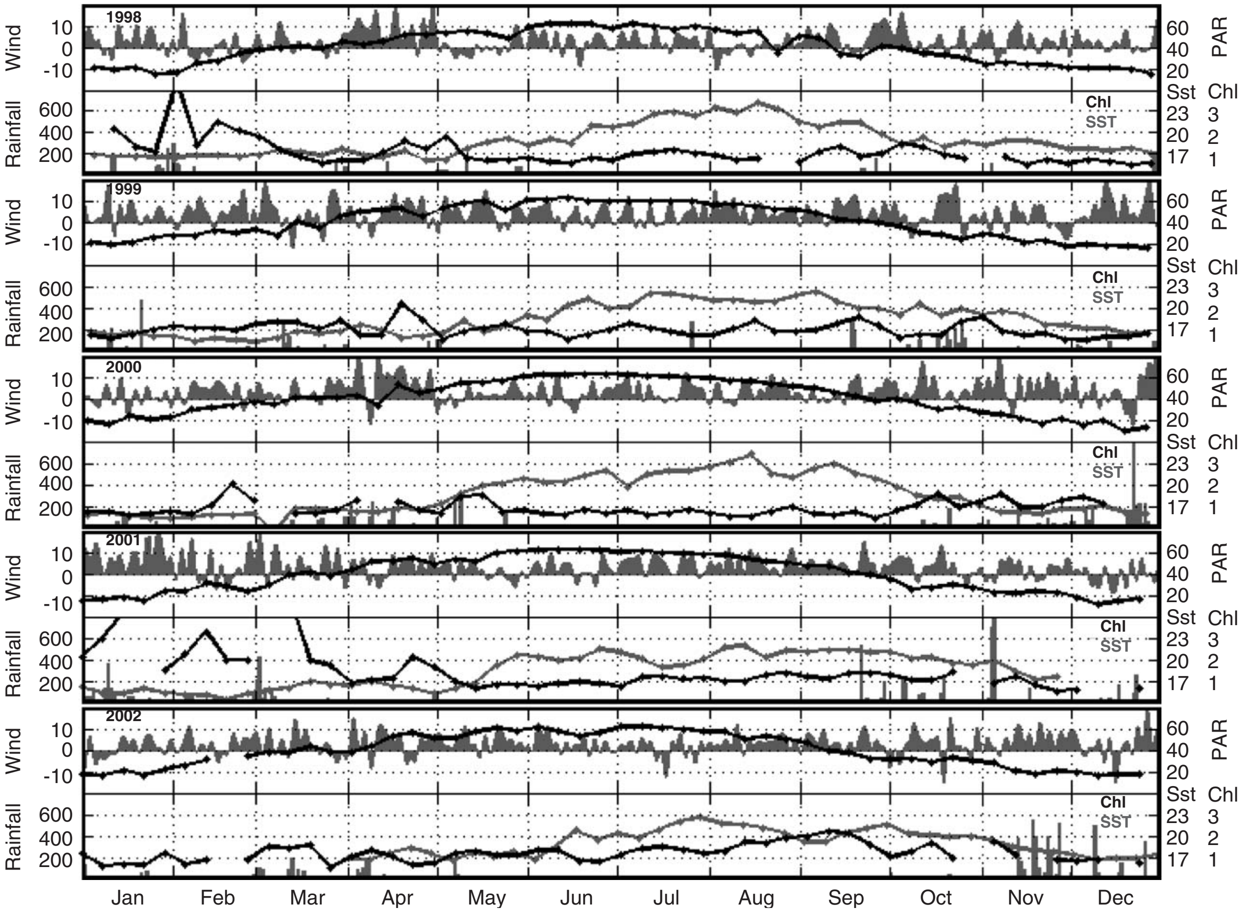

Fig. 13. Time series of local wind speed (grey bar) expressed as $km\,h^{-1}$ (positive values denotes westerlies and negative values correspond to easterlies) and PAR values (solid black line) in mol quanta $m^{-2}\,d^{-1}$ for the weekly composite in Zone 3 (top). Daily rainfall values (grey bar) in tenth $mm\,d^{-1}$ and chlorophyll concentration (black solid line) in $mg\,Chl\,m^{-3}$ and SST (grey solid line) in °C for weekly composite for Zone 3 (bottom).

was observed in association with weak winds. SST remained constant and strong rainfalls were registered, which possibly favoured the entrance of nutrients in the zone through the river discharge. This situation was also detected during October 2001 and November 2001.

3.1.5. Zone 5 or zone in Cape Trafalgar

Monthly SST climatology in Zone 5 (Fig. 7) displayed similar seasonal trends (Fig. 16). SST reached a maximum value of 21 °C in August and the minima were measured over February ($\approx$16 °C). The interannual variability was not as elevated as in the previous zone, due to the fact that the range of SST anomalies only varied $\pm$1 °C.

Monthly chlorophyll climatological series (Fig. 16) showed a similar pattern to that found in Zone 2, although with smaller concentrations. Two annual blooms were detected. A first one achieved in April ($\approx 1.1\,mg\,Chl\,m^{-3}$) and a second and more intense bloom reached in September ($\approx 1.3\,mg\,Chl\,m^{-3}$). The lowest chlorophyll concentration was detected in December ($\approx 0.8\,mg\,Chl\,m^{-3}$), although in June the chlorophyll concentration was also very low ($\approx 0.9\,mg\,Chl\,m^{-3}$). The interannual variability presented in this zone was very high and the anomalies represented almost 50% of the total chlorophyll concentration. In addition, the occurrence of these maxima took place over different periods depending on the year considered. As an example, the chlorophyll maximum was reached in April and September in 1998, whereas it was detected in March, May, August and October in 1999. The chlorophyll maximum was achieved in November

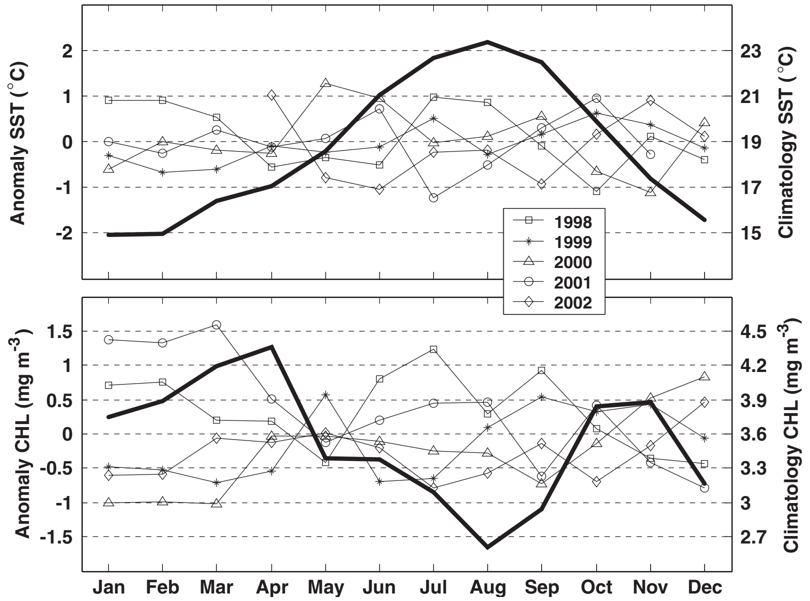

Fig. 14. Anomalies and climatology of SST (°C, top) and chlorophyll (mg Chl m^{-3}, bottom) of monthly composites between January 1998 and December 2002 for Zone 4. Climatology has been emphasized by the thick solid line.

and January in 2000 and 2001, respectively and in September for 2002.

Fig. 17 depicts the weekly mean of SST, PAR and chlorophyll concentration for Zone 5. SST was related with the fluctuations in chlorophyll concentration, since decreases in the former corresponded with rises in the latter. This situation could be an indication of the entrance of nutrients in the surface layer due to tide–topography interactions (Vargas-Yáñez et al., 2002). These interactions are subjected to temporal scales shorter than the weekly scale used in this study, and therefore they could not be detected. No clear relationships were observed between meteorological factors and the changes in chlorophyll.

4. Discusion

As indicated above, according to the second spatial mode of the EOF analysis several zones located in open and coastal regions could be identified in the Gulf of Cádiz. Zone 1 (open-ocean zone; Fig. 7) occupies an area of a bathymetry deeper than 1000 m; thereby the topography factor is not expected to greatly influence the physical and biological features. Following the Sverdrup model (Sverdrup, 1953), two annual blooms would be expected to occur in this area. Longhurst (1995, 1998) also described the possible appearance of two annual blooms at this latitude. However, results presented here showed only the occurrence of one maximum in winter. In particular, two main differences between the surface chlorophyll predicted by the Sverdrup model and that obtained in this study can be observed: (i) the bloom expected in spring was reached in winter instead; and (ii) the fall bloom was absent. Moreover, the pattern described for the oceanic zone is persistent in time. In fact, the chlorophyll estimations derived from CZCS (November 1979–June 1986) and Ocean Colour and Temperature Scanner (OCTS) (November 1996–June 1997) displayed the same regime as that observed by the SeaWiFS sensor (Fig. 18).

The occurrence of the winter bloom seems to be associated with a very deep mixed layer that allows the entrance of nutrients in the entire water column. This can be inferred when several temperature profiles measured in different oceanographic cruises carried out in the area are considered (see Fig. 13 in Navarro et al., 2006). According to the available data, the mixed layer exceeds 100 m depth during both February and March (see Vizconde-02-02 and Arsa-03-98 cruises, Fig. 13 in Navarro et al., 2006), causing mixing that permits the nutrient entrance in the surface layer. Also, the light intensity is sufficient to sustain phytoplankton growth and consequently generates the bloom. This can be demonstrated when daily depth-averages PAR

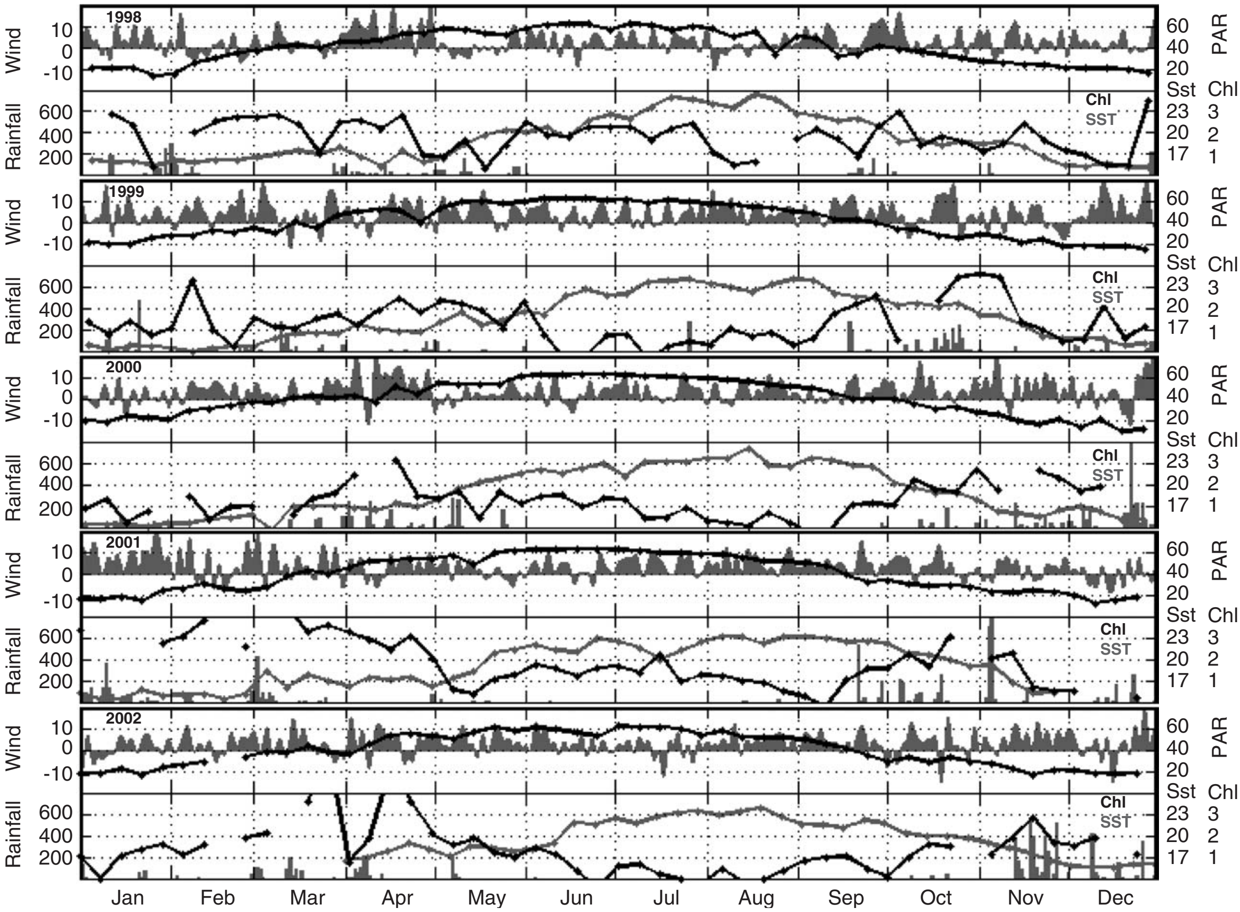

Fig. 15. Time series of local wind speed (grey bar) expressed as $km\,h^{-1}$ (positive values denotes westerlies and negative values correspond to easterlies) and PAR values (solid black line) in mol quanta $m^{-2}\,d^{-1}$ for the weekly composite in Zone 4 (top). Daily rainfall values (grey bar) in tenth mm d^{-1} and chlorophyll concentration (black solid line) in mg Chl m^{-3} and SST (grey solid line) in °C for weekly composite for Zone 4 (bottom).

values are calculated in this layer for February, using

$$I_m = \frac{\int_0^{Z_{MLD}} 0.6 E_0 e^{-K_d z} dz}{Z_{MLD}}, \quad (3)$$

where Z_{MLD} is mixed layer depth, E_0 is daily PAR intensity derived from the SeaWiFS data (Fig. 9) for that particular month ($30\,\mu E\,m^{-2}\,d^{-1}$), K_d is attenuation coefficient derived from in situ data (Navarro et al., 2006), and 0.6 is a factor that represents the loss of light in the air–water interphase integrated during whole day (Tett et al., 2002). For the Zone 1, the range of K_d was found to oscillate between 0.05 and $0.07\,m^{-1}$ (Navarro, 2004) and average PAR intensity for the upper 100 m was always higher than $2\,\mu E\,m^{-2}\,s^{-1}$ (Fig. 19), which is greater than the compensation intensity value calculated for the stations located in this zone (Navarro et al., 2006), although both values are very similar. Therefore, phytoplankton net growth was not limited by light although it is expected to be slow. Considering an α (initial slope of P–I curves) of 0.025 $(W\,m^{-2})^{-1}\,d^{-1}$ (Fasham et al., 1990), phytoplankton growth rate can be calculated at that light intensity of $2\,\mu E\,m^{-2}\,s^{-1}$ as the product of α and the average PAR intensity in the mixed layer. This estimation results in a rate of $0.0109\,d^{-1}$, which is far below the maximum $2.5\,d^{-1}$ that can be obtained at a temperature of 15 °C (Brush et al., 2002). With this growth rate, the duplication time surpasses 63 days. Consequently, in February PAR is high enough to support phytoplankton growth and leads to the generation of the late

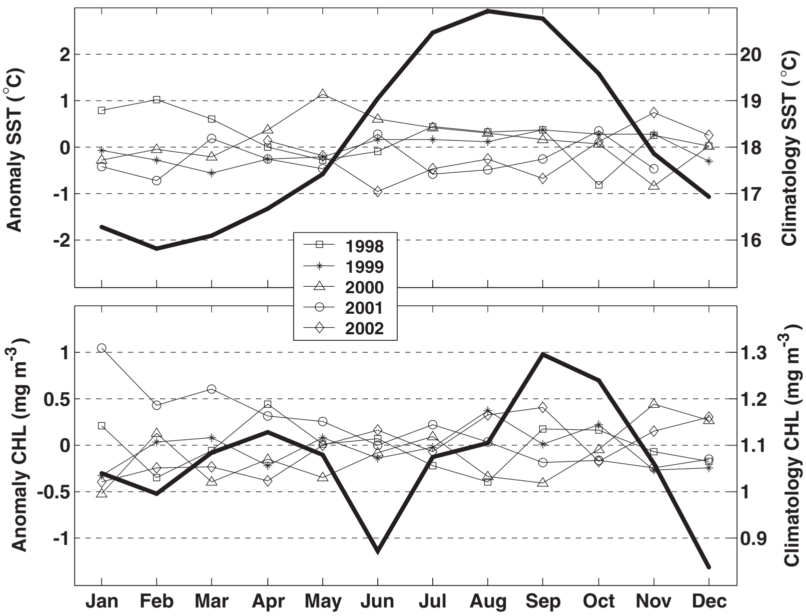

Fig. 16. Anomalies and climatology of SST (°C, top) and chlorophyll (mg Chl m^{-3}, bottom) of monthly composites between January 1998 and December 2002 for Zone 5. Climatology has been emphasized by the thick solid line.

winter bloom, even though the maximum of the chlorophyll concentration was not very high (≈0.35 mg Chl m^{-3}). When the seasonal thermocline develops, nutrient flow towards surface waters is prevented and surface chlorophyll diminishes, as it is observed in monthly climatology (Fig. 9). In addition, an increase in the deep chlorophyll maximum occurs during the stratification period, although this maximum cannot be detected by remote sensors. These findings are in agreement with others previously reported by Townsend et al. (1992) in the Atlantic Ocean. In that study the deep chlorophyll maxima can be originated before the thermocline formation, as a result of a reduction of mixing processes in the surface layer. In addition, studies described by Thomas et al. (2001) have established that the chlorophyll maxima appear in February–March in areas situated at the same latitude as the Gulf of Cádiz as well as in basins near our study area, such as the Portuguese coast (Peliz and Fiúza, 1999) and the Alborán Sea (García-Gorriz and Carr, 1999). Also, Yoder et al. (2001) obtained the same result tendency in the American east coast.

The absence of a fall bloom in the open ocean zone seems to be related to the depth of mixed-layer entrainment over this season. During the fall months, the nutricline depth is located around 90 m, whereas the mixed layer is sited at 50 m (for example Gulf-10-00 and Sesit-11-98, Fig. 13 in Navarro et al., 2006). The fact that the mixed layer is shallower than the nutricline depth does not allow nutrient injection in surface waters, and the second bloom does not appear in the open-sea zone during the season.

The relationship existing between the depths of both the mixed layer and the nutricline for the different zones in the Gulf of Cádiz and upwelling processes could explain the spring chlorophyll maximum detected in the rest of coastal zones. As the nutricline is shallower and exposed to high dynamic processes in the areas close the coast, nutrients can be introduced in the photic zone during the spring season, when PAR intensity is also greater. In summer and fall months, a second phytoplankton bloom appears, whose origin can lie in diverse processes. For instance, near Cape San Vicente (Zone 2; Fig. 7) and Cape Santa María (Zone 3; Fig. 7), wind plays an important role in the generation of upwelling (Fiúza et al., 1982; Fiúza, 1983). Generally, northly wind are known to produce upwelling on the west coast of Portugal, whereas westerlies are involved in the formation of upwelling on the south coast of Portugal. The presence of these winds, normally more persistent and stronger in summer (Fiúza et al., 1982), could

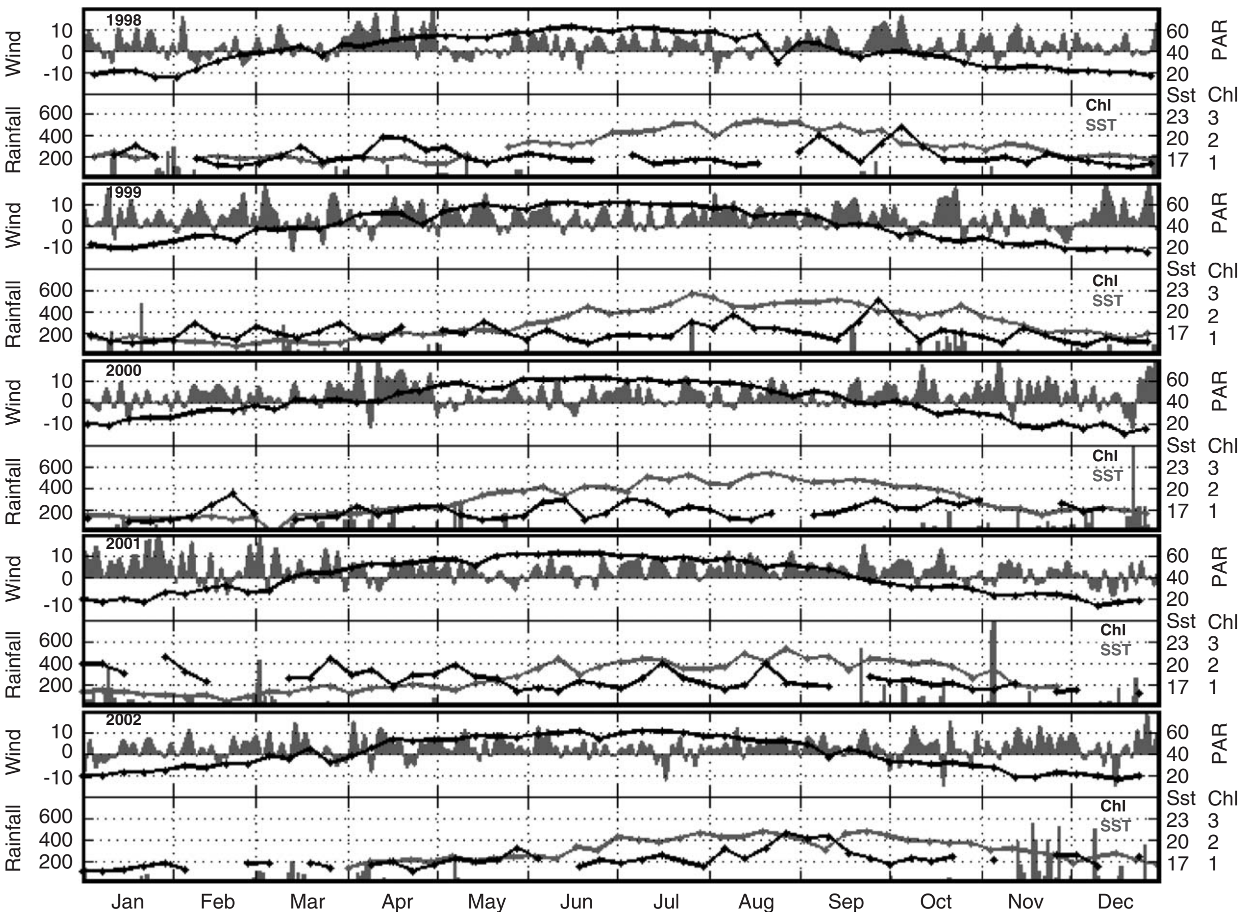

Fig. 17. Time series of local wind speed (grey bar) expressed as km h^{-1} (positive values denotes westerlies and negative values correspond to easterlies) and PAR values (solid black line) in mol quanta m^{-2} d^{-1} for the weekly composite in Zone 5 (top). Daily rainfall values (grey bar) in tenth mm d^{-1} and chlorophyll concentration (black solid line) in mg Chl m^{-3} and SST (grey solid line) in °C for weekly composite for Zone 5 (bottom).

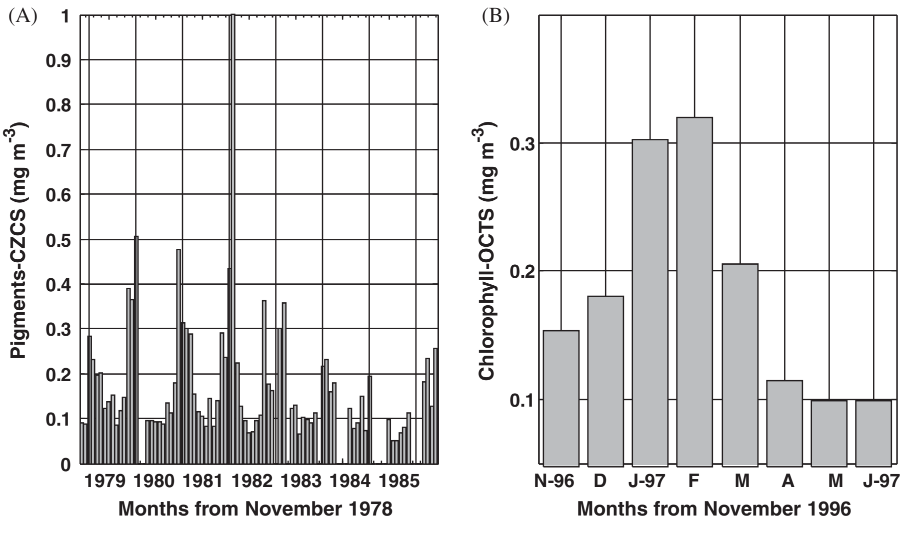

Fig. 18. (A) Monthly pigments concentration (mg m^{-3}) for Zone 1 detected by CZCS (between November 1979 and June 1986) and B) Monthly chlorophyll concentration (mg Chl m^{-3}) for Zone 1 detected by OCTS (between November 1996 and June 1997).

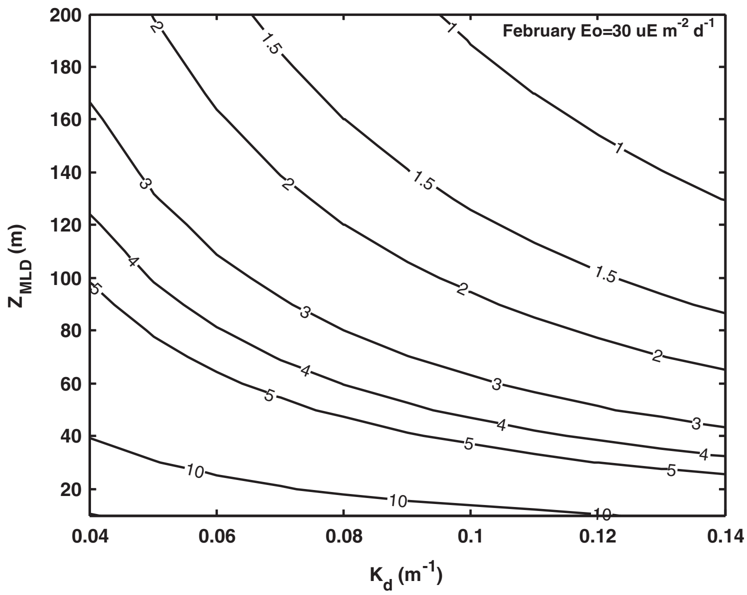

Fig. 19. Contour plots for the average intensity of PAR (μmol quanta $m^{-2} s^{-1}$) in the mixed layer during February ($E_0 = 30\,\mu E\,m^{-2}\,s^{-1}$) calculated at different values of $K_d\,(m^{-1})$ and for the different depths of the mixed layer (m).

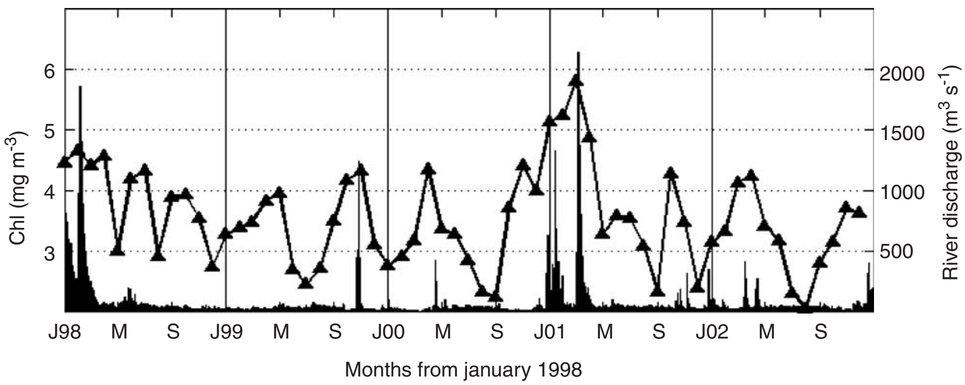

Fig. 20. Monthly chlorophyll concentration (triangle marks, mg Chl m^{-3}) for Zone 4. Thin line represents the river discharge in Alcalá del Río dam in ($m^3\,s^{-1}$).

explain the appearance of the chlorophyll maximum in both zones, as it is observed in monthly climatologies (Figs. 10 and 12, respectively). The intensity of the second maximum in Cape San Vicente was greater than that found in Cape Santa María, which can be attributed to the fact that the northlies around the former are more intense than around the latter (Fiúza et al., 1982).

The connection between westerlies and the presence of upwelling in Cape San Vicente can be observed in Fig. 11, where a decrease in SST coincides with an increase in the chlorophyll concentration. The upwelling is less intense in the south coast than in the west coast of Portugal (Sousa and Bricaud, 1992). Fig. 11 clearly shows cold water upwelled in Cape San Vicente during the summer months, where minimum SST is registered as compared with other areas in the vicinity. The upwelling of cold deep waters leads to the entrance of nutrients in surface waters, favouring phytoplankton growth and therefore a rise in chlorophyll concentration (Fig. 11). In this zone, filaments and eddies in the daily images of SST usually can be found (Relvas and Barton, 2002). Sousa and Bricaud (1992) expressed the particular interest of San Vicente region due to diversity of phytoplankton patterns detected in their study. They showed that although the persistence of these filaments is high, their directions and forms could be very variable. These SST filaments have a clear correspondence with chlorophyll filaments and can cause a considerable transport of pigments to oligotrophic zones of open sea, farther than 200 km (Sousa and Bricaud, 1992). Therefore, the filaments constitute an important source of primary production in the open ocean (Peliz and Fiúza, 1999; Peliz et al., 2004).

Zone 3 is located around the Huelva Front (Fig. 7). The formation of this cold front that is facilitated by westerlies (Vargas et al., 2003) produces an increase in the chlorophyll concentration in surface as a result of the nutrients entrance in surface layers, mainly during summer when the stratification of the water column is maxima. Moreover, because the nitrocline is located at shallower depths in this zone (Navarro et al., 2006), a weak wind could create a mixed layer deeper than the nitrocline depth, injecting nutrients into the photic zone. Sousa and Bricaud (1992) found that the Huelva Front constituted a quasi-permanent structure maintained between July and August in 1983. Our results (Fig. 13) support this finding, since over the summer period when stratification is very strong, westerlies are associated with diminutions in SST and increases in surface chlorophyll concentration. Sousa and Bricaud (1992) also reported this relationship and showed daily CZCS images in which a plume characterized by high pigments concentrations could be observed at the east of Cape Santa María.

The pattern of monthly chlorophyll in Cape Trafalgar (Zone 5; Fig. 16) is similar to that observed in Zone 2 (Fig. 10) or 3 (Fig. 12), with a spring maximum that corresponds to a typical spring bloom and a second maximum, of a greater magnitude, that occurs in summer. This second maximum, reached during the stratification period, seems to be related to the mixing occurring in this zone due to tide–topography interactions. (Vargas-Yañez et al., 2002). The interaction happens throughout the year, but it is in summer and fall when the interchange between the deep and surface layer is greater (Vargas-Yañez et al., 2002). As a result of the mixing, nutrient fertilization in surface layers takes place, with the subsequent rise in chlorophyll concentration that generates the second chlorophyll maximum in summer. In addition, this period of the year is characterized by high values of radiation that triggers phytoplankton growth. Fig. 17 indicates the relationship between the increase in the chlorophyll concentration and the reductions in SST throughout the different years considered.

Finally, in the coastal area (Zone 4, Fig. 7) a high relationship between physical and biological forcing can be observed. During the stratification period (between April and October, Sánchez-Lamadrid et al., 2003), the occurrence of easterlies coincides with diminutions in surface chlorophyll (Fig. 15) whereas when strong and prolonged westerlies blow, the concentration increases considerably. This pattern could be explained by the Ekman transport, since westerly forces the surface water to move towards the south and surface water is replaced by colder and more nutrient-rich bottom waters. In addition, the mixed layer formed by the wind stress can entrain a nutricline, which is forced to be shallow by the Ekman pumping. Fig. 15 also demonstrates that Zone 4 is affected by the rainfall. A rise in precipitation accompanied by a high river discharge increases presumably the nutrient concentration in this zone (Huertas et al., 2005), which produces an augment in chlorophyll concentration. Furthermore, heavy precipitations could explain the chlorophyll maximum detected in the beginning of fall. Fig. 20 shows that a high river discharge from the Alcala del Río dam (Fig. 1) in the course of the Guadalquivir River coincides with an increase of monthly chlorophyll concentration, probably due to the input of nutrients of a riverine origin to the ecosystem. In fact, the highest phytoplankton bloom registered in the continental shelf of the Gulf of Cádiz took place between January and March 2001, corresponding with the heaviest rainfall registered in the last 5 years. Peliz and Fiúza (1999) also pointed out a direct relationship between precipitation and chlorophyll concentration.

5. Concluding remarks

In summary, results presented in this study show that the temporal phytoplankton distribution in the Gulf of Cádiz could be explained by the relationship existing between the respective depths of both the mixed layer and the nutricline. In the open sea, the surface chlorophyll maxima occur in winter, when intense winds force the mixed layer to move deeper than the nutricline. However, in coastal areas, the chlorophyll maximum appears in spring followed by a second bloom either in summer or fall, mainly due to the presence of several processes that favour the nutrient entrance, such as upwelling events, river discharge, etc. In addition, the alternation between westerlies and easterlies influence the biological production in the basin, since the former causes an increase in chlorophyll concentration and the latter results in a marked decrease in phytoplankton biomass. Also rainfall and river discharge affect markedly chlorophyll concentration.

Acknowledgments

We are grateful to the DLR (German Remote Sensing Data Center) for providing the SST images and SeaWiFS Project (code 970.2) for SeaWiFS images. We also thank Dr. Osvaldo Ulloa (PROFC), Dr. Frank Muller-Karger (USF), Dr. Chuanmin Hu (USF) and other colleagues at the PROFC (University of Concepcion, Chile) and University of South Florida for help with SeaWiFS image processing. Two anonymous reviewers provided us with helpful comments to improve the manuscript. Consejería de Agricultura y Pesca de la Junta de Andalucía provided several in situ chlorophyll data. Remote sensing images have been processed in Ocean Color Remote Sensing Service at ICMAN-CSIC. This work was supported by the projects MAR99-0643-C03-02, VEM2004-08579 and CTM2005-01091/MAR (M.E.C.) and a F.P.I. fellowship to G.N.

References

Baldacci, A.G.C., Grasso, R., Manzella, G., Allen, J.T., Cipollini, P., Guymer, T.H., Snaith, H.M., 2001. A study of the Alboran sea mesoscale system by means of empirical orthogonal function decomposition of satellite data. Joural of Marine Syststems 29, 293–311.

Baringer, M.O., Price, J.F., 1999. A review of the physical oceanography of the Mediterranean outflow. Marine Geology 155 (1–2), 63–82.

Brickley, P.J., Thomas, A.C., 2004. Satellite-measured seasonal and inter-annual chlorophyll variability in the Northeast Pacific and Coastal Gulf of Alaska. Deep Sea Research II 51, 229–245.

Brush, M.J., Brawley, J.W., Nixon, S.W., Kremer, J.K., 2002. Modeling phytoplankton production: problems with the Eppley curve and an empirical alternative. Marine Ecology Prog. Series 238, 31–45.

Criado-Aldeanueva, F., García-Lafuente, J., Vargas, J.M., Del Río, J., Vázquez, A., Reul, A., Sánchez, A., 2006. Distribution and circulation of water masses in the Gulf of Cádiz from in situ observations. Deep Sea Research, this issue [doi:10.1016/j.dsr2.2006.04.012].

Davis, J.C., 1973. Statistics and data analysis in geology. Wiley, New York, (464pp).

Fasham, M.J.R., Ducklow, H.W., McKelvie, S.M., 1990. A nitrogen-based model of plankton dynamics in the oceanic mixed layer. Journal of Marine Research 48, 591–639.

Fiúza, A.F.D., de Macedo, M.E., Guerreiro, M.R., 1982. Climatological space and time variation of the Portuguese coastal upwelling. Oceanol. Acta 5 (1), 31–40.

Fiúza, A.F.D., 1983. Upwelling patterns off Portugal. In: Suess, E., Thiede, J. (Eds.), Coastal Upwelling. Plenum, New York, pp. 85–98.

Folkard, A.M., Davies, P., Fiúza, A.F.G., Ambar, I., 1997. Remotely sensed sea surface thermal patterrns in the Gulf of Cádiz and the Strait of Gibraltar: variability, correlations and relationships with the surface wind field. Journal of Geophysical Research 102 (C3), 5669–5683.

García, C.M., Prieto, L., Vargas, M., Echevarría, F., García-Lafuente, J., Ruiz, J., Rubin, J.P., 2002. Hydrodynamics and the spatial distribution of plankton and TEP in the Gulf of Cádiz (SW Iberian Peninsula). Journal of Plankton Research 24 (8), 817–833.

García-Gorriz, E., Carr, M.E., 1999. The climatological annual cycle of satellite-derived phytoplankton pigments in the Alboran Sea. Geophysical Research Letters 26 (19), 2985–2988.

García-Lafuente, J., Delgado, J., Criado-Aldeanueva, F., Bruno, M., Vargas, J.M., 2006. Water mass circulation on the continental shelf of the Gulf of Cádiz. Deep Sea Research II, this issue [doi:10.1016/j.dsr2.2006.04.011].

Ho, C.R., Zheng, Q., Kuoa, N.J., 2004. SeaWiFS observations of upwelling south of Madagascar: long-term variability and interaction with East Madagascar Current. Deep Sea Research II 51, 59–67.

Huertas, I.E., Navarro, G., Rodríguez-Gálvez, S., Prieto, L., 2005. The influence of phytoplankton biomass on the spatial distribution of carbon dioxide in the surface sea water of a coastal area of the Gulf of Cádiz (southwestern Spain). Canadian Journal of Botany 83, 929–940.

Kelly, K.A., 1988. Comment on "Empirical orthogonal function analysis of advanced very high resolution radiometer surface temperature patterns in Santa Barbara channel" by G.S.E. Lagerloef and R.L. Bernstein. Journal of Geophysical Research 93, 15753–15754.

Lagerloef, G.S., Bernstein, R.L., 1988. Empirical othogonal analysis of advanced very high resolution radiometer surface temperature patterns in Santa Barbara Channel. Journal of Geophysical Research 93, 6863–6873.

Lavender, S.J., Pinkerton, M.H., Froidefond, J.M., Morales, J., Aiken, J., Moore, J., 2004. G.F. SeaWiFS validation in European coastal waters using optical and bio-geochemical measurements. International Journal of Remote Sensing 25 (7–8), 1481–1488.

Lorenz, E.N., 1956. Empirical orthogonal functions and statistical weather prediction. Sci. Rep. No. 1, Statist. Forecasting Proj., Department Meteor., MIT (49pp).

Longhurst, A.R., 1995. Seasonal cycles of pelagic production and consumption. Prog. Oceanogr. 36, 77–167.

Longhurst, A.R., 1998. Ecological Geography of the Sea. Academic Press, San Diego, (398pp).

McClain, E.P., Pichel, W.G., Walton, C.C., 1985. Comparative performance of AVHRR based multichannel sea surface temperatures. Journal of Geophysical Research 90, 11587–11601.

McClain, C.R., Arrigo, K.R., Esaias, W.E., Darzi, M., Patt, F.S., Evans, R.H., Brown, J.W., Brown, C.W., Barnes, R.A., Kumar, L., 1995. SeaWiFS algorithms, Part 1. NASA technical memorandum 104566. In: Hooker, S.B., Firestone, E.R., Acker, J.G. (Eds.), NASA Goddard Space Flight Center, vol. 28. Greenbelt, Maryland, p. 46.

Navarro, G. 2004. Escalas de variabilidad espacio-temporal de procesos pelágicos en el golfo de Cádiz, PhD, University of Cádiz (224pp).

Navarro G., Ruiz, J., Huertas, I.E., García, C.M., Criado-Aldeanueva, F., Echevarría, F., 2006. Basin scale structures governing the position of the deep fluorescence maximum in the Gulf of Cádiz. Deep Sea Research II, this issue [doi:10.1016/j.dsr2.2006.04.013].

North, G.R., Bell, T.L., Cahalan, R.F., Moeng, F.J., 1982. Sampling errors in the estimation of empirical orthogonal functions. Monthly Weather Review 110, 699–706.

O'Reilly, J.E., Maritonera, S., Mitchell, B.G., Siegel, D.A., Carder, K.L., Garver, S.A., Kahru, M., McClain, C.R., 1998. Ocean color chlorophyll algorithms for SeaWiFs. Journal of Geophysical Research 103 (C11), 24937–24953.

O'Reilly, J.E., and 24 Coauthors, 2000. In: Hooker, S.B., Firestone, E.R. (Eds.), SeaWiFS Postlaunch Calibration and Validation Analyses, Part 3. NASA Tech. Memo. 2000-206892, vol. 11, NASA Goddard Space Flight Center, 49pp.

Palacios, D.M., 2004. Seasonal patterns of sea-surface temperature and ocean color around the Galápagos: regional and local influences. Deep-Sea Research II 51, 43–57.

Parada, M., Canton, M., 1998. Sea surface temperature variability in Alborán Sea from satellite data. International Journal of Remote Sensing 19 (13), 2439–2450.

Peliz, A.J., Fiúza, A.F.G., 1999. Temporal and spatial variability of CZCS-derived phytoplankton pigment concentrations off the western Iberian Peninsula. International Journal of Remote Sensing 20 (7), 1363–1403.

Peliz, A., Santos, A.M.P., Oliveira, P.B., Dubert, J., 2004. Cross-shelf transport induced by eddy interaction at the southwest of Iberian Peninsula in February 2001. 4[a] Asambleia Luso-Espanhola de Geodesia e Geofisica, Figueira da Foz, 2004.

Prieto, L., García, C.M., Corzo, A., Ruiz, J., Echevarría, F., 1999. Phytoplankton, bacterioplankton and nitrate reductase activity distribution in relation to physical structure in the northern Alborán Sea and Gulf of Cádiz (southern Iberian Península). Boletin del Instituto Espanol Oceanografia 15, 401–411.

Relvas, P., Barton, E.D., 2002. Mesoscale patterns in the Cape Sao Vicente (Iberian Peninsula) upwelling region. Journal of Geophysical Research 107 (C10), 3164.

Sánchez-Lamadrid, A., Ruiz, J., García E., Juárez, A., Jiménez, T., Sobrino, I., Blanco, E., Jiménez, P., Bruno, M., Navarro, G. 2003. Estudio de los recursos pesqueros del Golfo de Cádiz, Consejería de Agricultura y Pesca, Junta de Andalucía.

Sousa, F., Bricaud, A., 1992. Satellite-derived phytoplankton pigments structures in the portuguese upweling area. Journal of Geophysical Research 97 (C7), 11343–11356.

Stevenson, R.E., 1977. Huelva Front and Malaga, Spain, Eddy Chain as defined by Satellite and Oceanographic Data. Deutsche Hydrographische Zeitschrift 30 (2), 51–53.

Sverdrup, H.U., 1953. On the conditions for vernal blooming of the phytoplankton. Journal du Conseil Permanente Internationale pour lÉxploration de la Mer 18, 287–295.

Tett, P., Arístegui, J., Barton, E.D., Basterretxea, G., De Armas, J.D., Escánez, J.E., Hernández-León, S., Lorenzo, L.M., Montero, N., 2002. Steady-state DCM dynamics in Canaries waters. Deep Sea Research (II) 49 (17), 3543–3559.

Thomas, A.C., Carr, M.E., Strub, P.T., 2001. Chlorophyll variability in Eastern Boundary Currents. Geophysical Research Letters 28 (18), 3421–3424.

Townsend, D.W., Keller, M.D., Sieracki, M.E., Acklezon, S.G., 1992. Spring phytoplankton blooms in the absence of vertical water column stratification. Nature 360, 59–62.

UNESCO, 1994. Protocols for joint global ocean carbon flux study (JGOFS) core measurements, Manuals and Guides, vol. 29 (170pp).

Vargas, J.M., García-Lafuente, J., Delgado, J., Criado, F., 2003. Seasonal and wind-induced variability of sea surface temperature patterns in the Gulf of Cádiz. Journal of Marine Syststems 38 (3–4), 205–219.

Vargas-Yáñez, M., Sarhan, T., Plaza, F., Rubin, J.P., García-Martínez, M.C., 2002. The influence of tide-topography interaction on low-frequency heat and nutrient fluxes. Application to Cape Trafalgar. Continental Shelf Research 22, 115–139.

Yoder, J.A., O'Reilly, J.E., Barnard, A.H., Moore, T.S., Ruhsam, C.M., 2001. Variability in coastal zone color scanner (CZCS) Chlorophyll imagery of ocean margin waters off the US East Coast. Continental Shelf Research 21, 1191–1218.